



ISSN 0975-413X
CODEN (USA): PCHHAX

Der Pharma Chemica, 2016, 8(13):200-213
(<http://derpharmachemica.com/archive.html>)

The inhibition effect of imidazopyridine derivatives on C38 steel in hydrochloric acid solution

R. Salim^{1,2}, E. Ech Chihbi^{1,2}, H. Oudda², Y. ELAoufir^{1,3}, F. El-Hajjaji¹, A. Elaattiaoui³,
A. Oussaid³, B. Hammouti⁴, H. Elmsellem⁴ and M. Taleb¹

¹Laboratoire des Procédés de Séparation, Faculté des Sciences, Kenitra (LPS) Faculté des Sciences Kénitra, Université Ibn Tofail Maroc.

²Laboratoire d'Ingénierie d'Electrochimie, Modélisation et d'Environnement (LIEME), Faculté des sciences/Université Sidi Mohammed Ben Abdellah, Fès, Maroc.

³Laboratory of Materials, nanotechnology et environnement. Faculty of Sciences, University of Mohammed V, Rabat, IbnBattouta, BP 1014 Rabat, Morocco.

⁴Laboratoire de chimie analytique appliquée, matériaux et environnement (LC2AME), Faculté des Sciences, B.P. 717, 60000 Oujda, Morocco.

ABSTRACT

The inhibition efficiencies of a new derivatives of imidazopyridine namely 7-méthyl- 2-phenyl imidazo [1,2-a]pyridine-3-carbaldehyde, 6-chloro-2-(4-fluorophenyl)imidazo[1,2-a]pyridine and 6,8-dibromo-2-phenylimidazo [1,2-a]pyridine on corrosion of carbon steel in hydrochloric acid solution was investigated by weight loss, potentiodynamic polarization and electrochemical impedance spectroscopy (EIS). The experimental results obtained by Gravimetric method showed that these compounds are good inhibitors for our steel. It were achieved an inhibition efficiencies in the range 90.28–95.69% for $10^{-3}M$ at 298K which decreased with decreasing of the inhibitors concentrations. There adsorption on the steel surface according to the Langmuir isotherm model and it's selected into a mixed-type. The results of gravimetric method are in good agreement with Electrochemical Impedance Spectroscopy (EIS) methods.

Keywords: corrosion, imidazopyridine, efficiencies, adsorption.

INTRODUCTION

The acid solution especially hydrochloric acid is widely used in many industrial processes because of their special chemical properties for picking, cleaning and descaling the metallic installation. [1-3] As consequences, the damages caused by application of this acid are not only the high cost for inspecting, repairing and replacement but constitute also a public risk. [4]

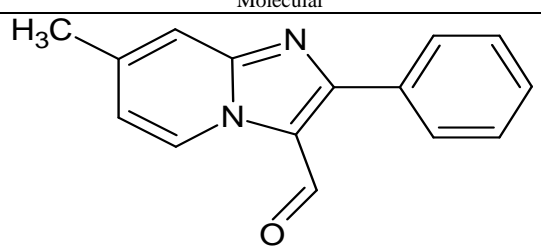
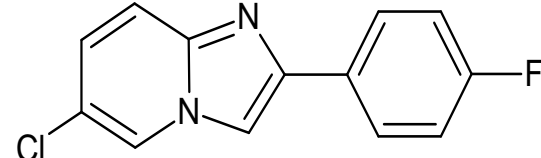
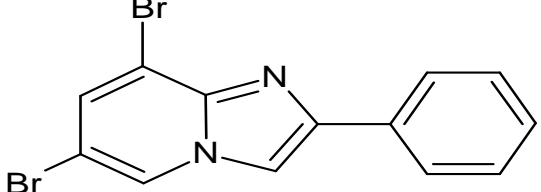
The most effective and preferred option to day is to affect the solution in place of the metal by using the inhibitors in order to reduce the acid attack and protection aspects. [5] A large number of inhibitors used at the present are organic compounds[6-10].It's containing heteroatom such as sulphur, phosphorus, nitrogen, oxygen, also when was had an aromatic ring and conjugate π double or triple bonds[11-14].

The adsorption of inhibitors depends to the nature and surface charge of metal, the electrolyte used and the chemical structure of the inhibitors[15].

The imidazopyridine derivatives are important molecular used in pharmaceutical industry such as antiviral, anti-inflammatory, and antibacterial [16]. Beside this, there are considered one of the most organic compounds such as pyrazole[17-18], imidazole [19-20] and pyridine [21-23] which demonstrated that they are excellent inhibitors against corrosion of metal.

The objective of this investigation is to determine the inhibition efficiency of three imidazopyridine derivatives namely 7-methyl- 2-phenyl imidazo [1,2-a]pyridne-3-carbaldehyde, 6-chloro-2-(4-fluorophenyl)imidazo[1,2-a]pyridine and 6,8-dibromo-2-phenylimidazo[1,2-a]pyridine Shown in table1 as new synthesized product on mild steel corrosion in 1M HCl. This investigation was conducted by weight loss measurements and electrochemical methods which carried out to study the mechanism of corrosion inhibition .the thermodynamic and kinetic characterization is obtained and discussed.

Table 1.molecular structures, name and abbreviations of studied imidazopyridine derivatives

Molecular	Name	Abbreviation
	7-methyl- 2-phenyl imidazo [1,2-a]pyridne-3-carbaldehyde	P1
	6-chloro-2-(4-fluorophenyl)imidazo[1,2-a]pyridine	P2
	6,8-dibromo-2-phenylimidazo[1,2-a]pyridine	P3

MATERIALS AND METHODS

2.1. Material preparation

The corrosion tests were performed on a mild steel containing (in wt %) 99.21 Fe, 0.38 Si, 0.21 C, 0.05 Mn, 0.05 S, 0.09 P and 0.01 Al. the surface of the specimens used was mechanically polished with different grade of emery paper (from 180 to 1200), rinsing with double distilled water, degreasing in acetone and drying before being immersed in the acid solution. the hydrochloric solution acid 1M was prepared by dilution of analytical grade 37% . the concentrations of inhibitors used in HCl 1M was 10^{-6} M- 10^{-3} M.

2.2.Weight loss measurements

Weight loss measurement carried out by weighing the mild steel before and after immersion in acid solution which contains a various concentration of inhibitor used. The experiments were performed in a cell equipped with a thermostated cooling condenser at different temperatures (308K, 318K, 328K and 338K) in solution prepared.

2.3. Electrochemical test

The electrochemical studies were performed by using a potentiostat Tacussel- Radiometer PGZ 100 and controlled by analysis software model voltmaster 4. The experiment was carried out a conventional of three electrode glass cell. The specimen was used as the working electrode, a saturated calomel electrode (SCEs) as the reference electrode and a platinum wire as the counter electrode. The working electrode was in the form of a square with exposed surface area 1 cm² which was subsequently ground with 1200 grit grinding papers, cleaned by distilled water, degreased with acetone

The working electrode was immersed in solution tested during 30 min until obtained the open circuit potential. The polarization curve was recorded from -700 to -200 mV/SCE with a scan rate of 1 mV.S-1. Firstly, the cathodic branch was determined then the anodic branch after re-established of the open circuit.

The impedance spectroscopy measurements recorded at the open circuit potential in the frequency range from 100 KHz to 10mHz. The impedance spectra are a semicircle represented in the Nyquist diagram.

2.4. Scanning electron microscopic

The surface morphology of the steel samples in the absence and presence of P1, P2 and P3 was investigated after immersion time in 1 M HCl solution using SEM (FEI COMPANY QUANTA 200).

RESULTS AND DISCUSSION

3.1. Gravimetric measurement

3.1.1. Effect of concentration

The evolution of corrosion rate before and after addition of inhibitors studied on C38 steel in HCl 1M was decided by weight loss measurement for 6h of immersion at 298K. The values calculated of W_{corr} and the inhibition efficiency (Ew %) determined by the following equation [24] :

$$W_{corr} = \frac{\Delta m}{S.T} \quad (1)$$

$$E\% = \frac{W_{corr} - W_{inh}}{W_{corr}} * 100 \quad (2)$$

W_{corr} and W_{inh} are the corrosion rate of steel without and with each inhibitor, respectively.

Table 2. Corrosion rate of steel in 1M HCl with and without inhibitors at various concentrations, and the corresponding inhibition efficiency

Inhibitor	Concentration (mol.l ⁻¹)	W_{corr} (mg.cm ⁻² .h ⁻¹)	IE (%)	θ
HCl 1M	--	0.6521	--	--
P1	10-6	0.3911	40.02	0.400
	10-5	0.3056	53.12	0.531
	10-4	0.1593	75.56	0.755
	10-3	0.0633	90.28	0.902
P2	10-6	0.2838	56.47	0.564
	10-5	0.1991	69.46	0.694
	10-4	0.1285	80.29	0.802
	10-3	0.0478	92.65	0.926
P3	10-6	0.2716	58.34	0.583
	10-5	0.2197	66.29	0.662
	10-4	0.0657	89.91	0.899
	10-3	0.0280	95.69	0.956

The plot of the corrosion rate versus concentration displayed in figure 1 shows that the highest efficiency in the present work condition was obtained with a concentration of 10⁻³ M for all inhibitors and its decrease with decreasing of concentration.

On the other hand, the variation of inhibition efficiency with concentration of inhibitors is plotted in figure 2; showing an opposite trend compared to the corrosion rate. In fact, a significant increase of (IE %) is obtained upon addition of quite low concentrations of inhibitors and reaches the highest value to 95.69%, 92.65% and 90.28% in the concentration of 10⁻³M.

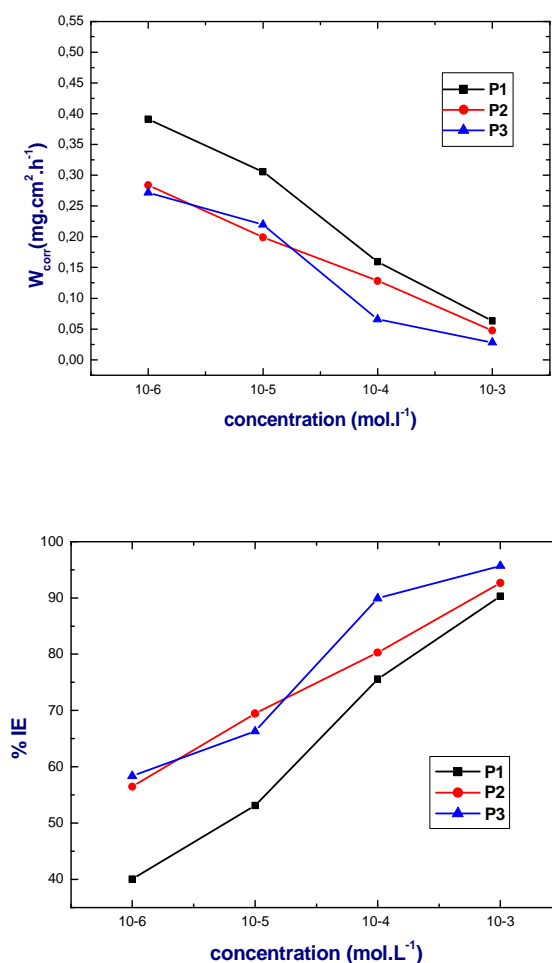


Figure 1 & 2 illustrate the variation of corrosion rate and efficiencies with concentration of inhibitor

• Adsorption isotherm

The adsorption isotherm is important to give us information about the interaction between the inhibitor and mild steel surface. This adsorption depends on several parameters such as the nature and charge of the corroding metal, the inhibitor's chemical structure and the charge distribution in the inhibitor's molecule. For our inhibitors a several adsorption isotherms are assessed but the best fitted straight line is obtained from the plot of C_{inh}/θ versus C_{inh} with slopes around unity.

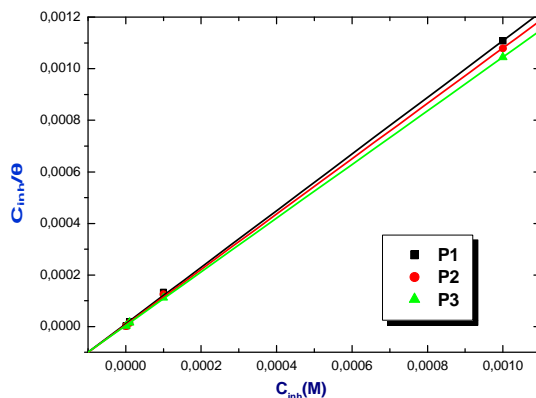


Figure 3. Langmuir adsorption isotherm of P1, P2 and P3 on carbon steel surface in 1 M HCl at 298 K

As a result our inhibitors were obeyed to the Langmuir's adsorption isotherm by following equation [25]:

$$\frac{C_{inh}}{\theta} = \frac{1}{K_{ads}} + C_{inh} \quad (3) \quad \text{with} \quad K_{ads} = \frac{1}{55.5} \exp\left(-\frac{\Delta_{ads}G^\circ}{RT}\right) \quad (4)$$

Where K_{ads} is the adsorption equilibrium constant and ΔG°_{ads} is the standard free energy of adsorption, 55.5 is a value of the molar concentration of water in the solution [26]

Table 3. Thermodynamic parameters for the adsorption of P1, P2 and P3 onto the mild steel surface in 1 M HCl at 298K

Inhibitor	slope	K_{ads} (L.mol ⁻¹)	R ²	$\Delta_{ads}G^\circ$ (KJ.mol ⁻¹)
P1	1.09	9,83.10 ⁴	0.999	-39,75
P2	1.07	1,46.10 ⁴	0.999	-42,08
P3	1.04	1,14.10 ⁴	0.999	-44,85

Table 3 summarizes the equilibrium constant and free energy of adsorption values. The negative values of standard free energy of adsorption ΔG°_{ads} ensure the spontaneity of adsorption process [27] and stability of the adsorbed layer on the steel surface. It is show that the calculated ΔG°_{ads} values, is ranging from -44.85 to -39.75 kJ mol⁻¹, indicating, therefore, that the adsorption mechanism of the inhibitors tested on mild steel surface in 1 M HCl solution as typical of chemisorptions. The possible mechanisms for chemisorptions can be attributed to the donation π -electron by the aromatic rings; the nonbinding electron pair of two nitrogen of imidazopyridine derive.

3.1.2. Effect of temperature

The temperature can change the interaction between mild steel and acidic solution with or without inhibitors. Generally the corrosion rate increases with the rise of temperature. At the present study, weight loss measurements are taken at range of temperature 308-338K in the absence and present of inhibitors during 2h of immersion and the corresponding results shown in table 4.

Table 4. Influence of temperature on the corrosion rate and inhibition efficiency of mild steel in 1 M HCl at different concentrations of P1, P2 and P3

Temperature (K)	Concentration (M)	P1		P2		P3	
		W_{corr} (mg cm ⁻² h ⁻¹)	IE (%)	W_{corr} (mg cm ⁻² h ⁻¹)	IE (%)	W_{corr} (mg cm ⁻² h ⁻¹)	IE (%)
308	--	1,2187	--	1,2187	--	1,2187	--
	10 ⁻³	0,1559	87,20	0,1459	88,02	0,0687	94,36
	10 ⁻⁴	0,3332	72,66	0,3009	75,30	0,2139	82,44
	10 ⁻⁵	0,6146	49,56	0,4635	61,96	0,4966	59,24
	10 ⁻⁶	0,7891	35,25	0,7527	38,24	0,6949	42,98
318	--	1,8312	--	1,8312	--	1,8312	--
	10 ⁻³	0,3066	83,25	0,3081	83,17	0,1230	93,28
	10 ⁻⁴	0,6821	62,74	0,6354	65,29	0,4869	73,40
	10 ⁻⁵	1,1673	36,25	0,8982	50,94	0,9689	47,09
	10 ⁻⁶	1,2338	32,62	1,3293	27,40	1,1423	37,61
328	--	2,7430	--	2,7430	--	2,7430	--
	10 ⁻³	0,5606	79,56	0,5901	78,48	0,2878	89,50
	10 ⁻⁴	1,3528	50,67	1,1799	56,98	0,9469	65,47
	10 ⁻⁵	1,9381	29,34	1,7206	37,27	1,6246	40,77
	10 ⁻⁶	2,0883	23,86	2,1382	22,04	2,0791	24,20
338	--	4,5291	--	4,5291	--	4,5291	--
	10 ⁻³	1,1350	74,93	1,2657	72,05	0,6891	84,78
	10 ⁻⁴	2,4857	45,11	2,2148	51,09	1,8725	58,65
	10 ⁻⁵	3,4698	23,38	3,3473	26,09	3,1200	31,11
	10 ⁻⁶	3,9210	13,42	4,0473	10,63	3,7429	17,35

As can be seen from the table 5, the corrosion rate at fixed temperature, decrease with increasing of concentration for the three inhibitors. Moreover, it is increase with the rise of temperature both in inhibited and uninhibited solutions. In other side, the inhibition efficiencies of each inhibitor decrease slightly with increasing of temperature to attain **74.93%** for P1, **72.05%** for P2 and **84.78%** for P3 at 10⁻³M in 338K which explain the figure 4. This result indicate that the higher temperature dissolution of steel predominates on adsorption of inhibitors studies at the metal.

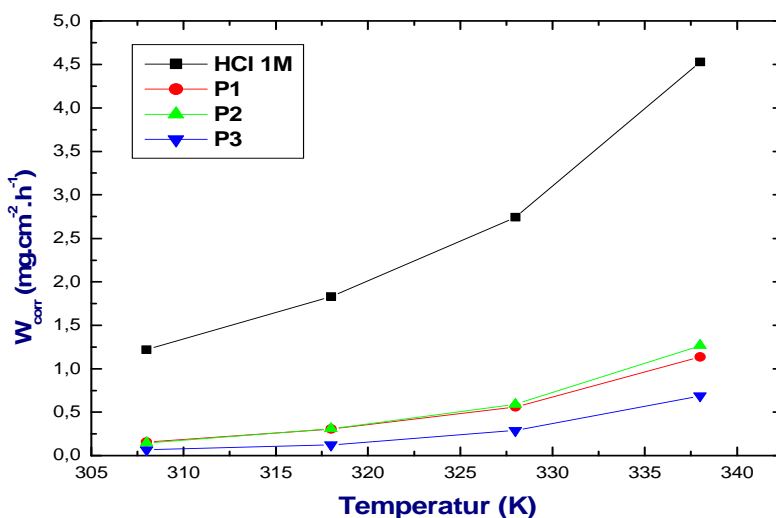


Figure 4. Variation of corrosion rate with temperature for mild steel in 1 M HCl in the presence of 10⁻³M of P1, P2 and P3

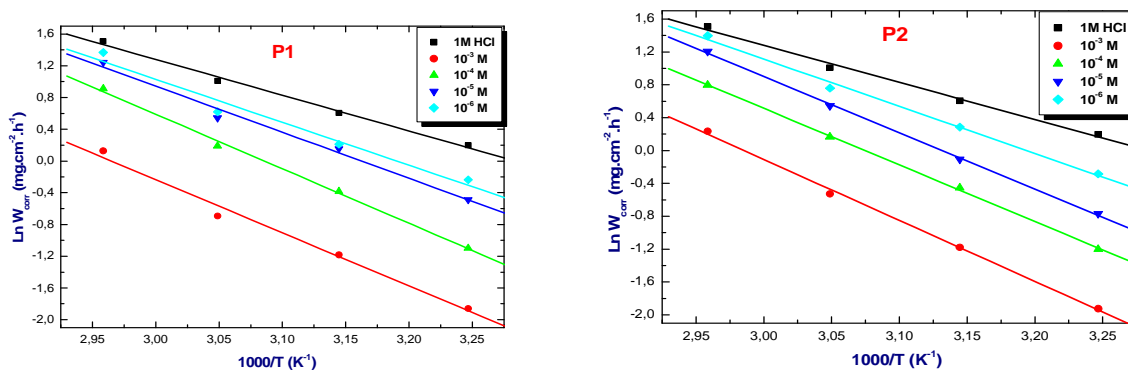
Inspection of Table 4 and figure 4 showed that corrosion rate increased with increasing temperature both in uninhibited and inhibited solutions while the inhibition efficiency of three inhibitor temperature. A decrease in inhibition efficiencies with the increase temperature in presence of the inhibitors might be due to weakening of physical adsorption.

The influence of temperature on the kinetic corrosion process leads to get more information about adsorption of inhibitors on metallic materials. In order to calculate activation parameters for the corrosion process, Arrhenius Eq. (5) and transition state Eq. (6) were used [28]:

$$W_{corr} = Ae^{\left(\frac{-E_a}{RT}\right)} \tag{5}$$

$$W = \frac{RT}{Nh} \exp\left(\frac{\Delta S^*}{R}\right) \exp\left(-\frac{\Delta H^*}{RT}\right) \tag{6}$$

Where W_{corr} is the corrosion rate, R the gas constant, T the absolute temperature, A the pre-exponential factor, h the Plank's constant and N is Avogrado's number, E_a the activation energy for corrosion process, ΔH^* the enthalpy of activation and ΔS^* the entropy of activation.



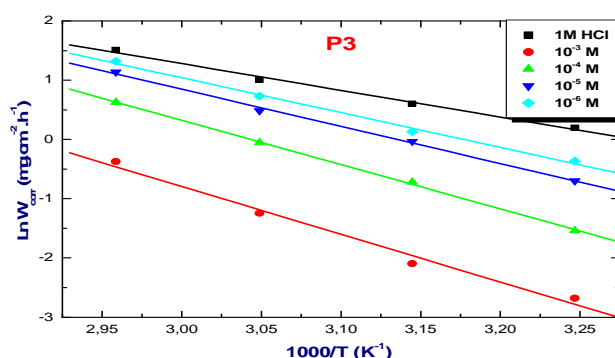


Figure 5. Arrhenius plots of mild steel in 1 M HCl at different concentrations of P1, P2 and P3

The apparent activation energy was determined from the slopes of logarithm of corrosion rate versus $10^3/T$ graph depicted in Figure 5. The intercepts of the lines permit the calculation of the values of the pre-exponential factor (A) and the slopes which equal $(-E_a/RT)$ allowed the determination of the activation energy (E_a).

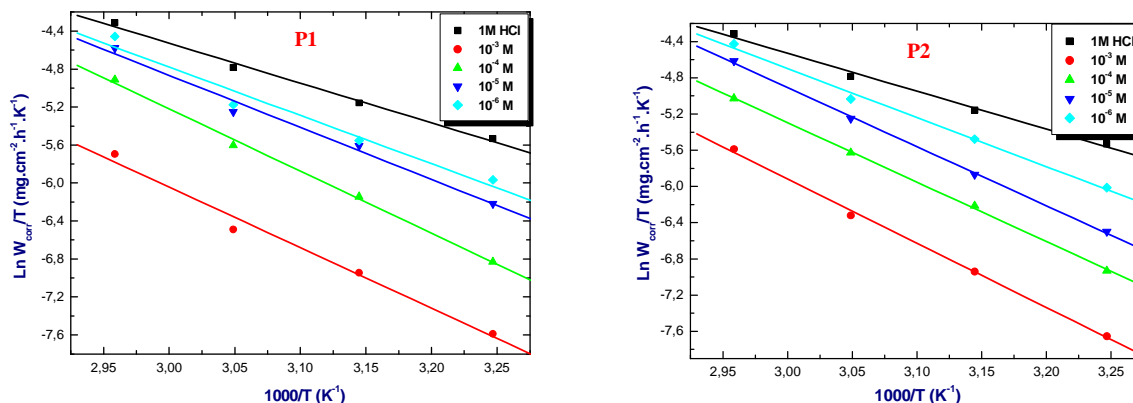
In other hand, the values of enthalpy and entropy of activation determined from the Plots of $\text{Log}(w_{\text{corr}}/T)$ vs. $10^3/T$ give a straight line with a slope of $\Delta H^\circ/R$ and an intercept of $(\text{Log}(R/Nh) + \Delta S^\circ/R)$ as shown in Fig. 6

The calculated parameters in the absence and presence of inhibitors are regrouped in Table 5.

Table 5. Activation parameters E_a , ΔH° and ΔS° of mild steel dissolution in 1 M HCl in the absence and in the presence of P1, P2 and P3 at different concentrations

Concentration (M)	E_a (kJ.mol ⁻¹)			ΔH° (kJ.mol ⁻¹)			ΔS° (J.K ⁻¹ .mol ⁻¹)		
	P1	P2	P3	P1	P2	P3	P1	P2	P3
HCl 1M	37,53			34,85			-142,70		
10 ⁻³	55,69	61,72	67,06	53,02	59,04	64,38	-100,82	-81,71	-71,37
10 ⁻⁴	57,13	57,25	62,16	54,45	54,57	59,48	-89,66	-89,94	-76,78
10 ⁻⁵	48,29	56,96	52,20	45,61	54,28	49,52	-113,25	-87,57	-102,29
10 ⁻⁶	45,01	47,76	48,86	42,33	45,08	46,18	-122,35	-113,43	-110,72

Inspection of Table 5 showed that the value of E_a determined in 1M HCl containing inhibitors is higher than uninhibited solution for the three inhibitors. The increase in the apparent activation energy may be interpreted as physical adsorption that occurs in the first stage [29]. Popova et al. [30] pointed out that the decrease of inhibition efficiencies may be attributed to the specific interaction between the iron surface and the inhibitor components. The change of the values of the apparent activation energies may be explained by the modification of the mechanism of the corrosion process in the presence of adsorbed inhibitor molecules [31] and could be often interpreted as an indication for the formation of an adsorptive film by a physical (electrostatic) mechanism [29].



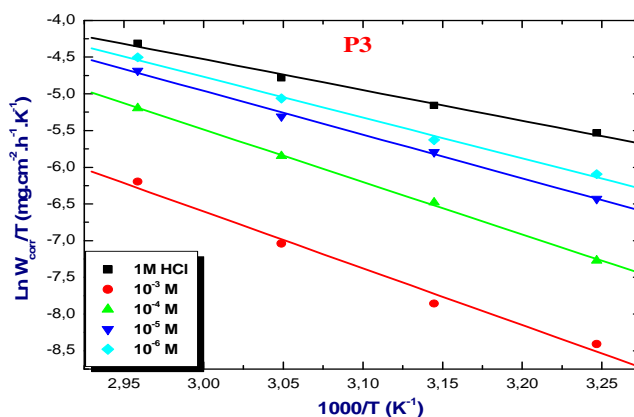


Figure 6. Arrhenius plots of $\ln W_{\text{corr}}/T$ versus $1000/T$ at different concentrations of P1, P2 and P3

The positive sign of the enthalpies ΔH° reflect the endothermic nature of the steel dissolution process and mean that the dissolution of carbon steel is difficult also, the increases of ΔS° is generally interpreted as an increase in disorder as the reactants are converted to the activated complexes [32].

In this study our inhibitors reflect an endothermic nature and the values of ΔS° increases negatively with the presence of the inhibitor than the non-inhibited one, reflecting the formation of an ordered stable layer of inhibitor on the steel surface. As was trace the isotherm adsorption in the effect of concentration, the ones of effect of temperature are represented in figure 7 which also obtained with Langmuir isotherm. As a result the parameter of equilibrium constant and standard free energy regrouped in table 6.

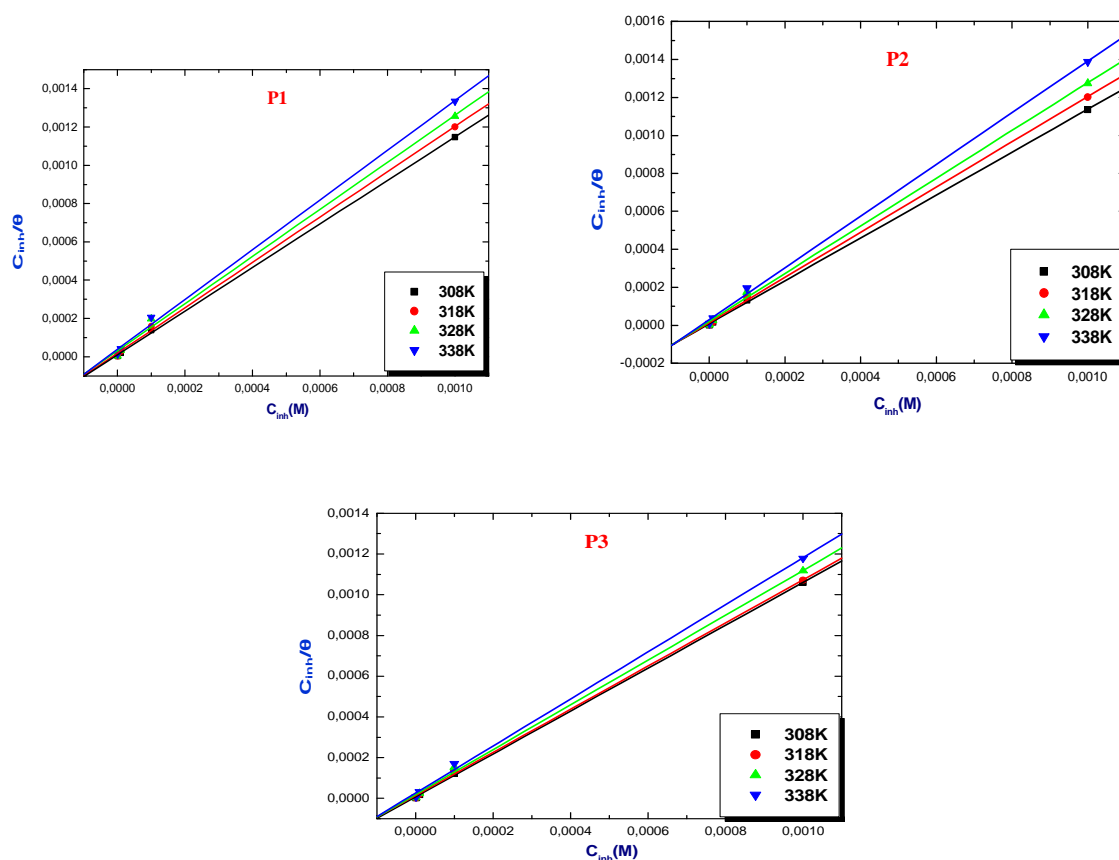


Figure 7. Langmuir isotherm adsorption model on the steel surface for P1, P2 and P3 in 1 M HCl

As we seen in effect of concentration, the values of free energy $\Delta_{\text{ads}}G^\circ$ in the rise of temperature are around of 40KJ.mol^{-1} which explains the nature chemisorption of three inhibitors.

Table 6. Thermodynamic parameters for the adsorption of P1, P2 and P3 on C38 steel at different temperatures

Inhibitor	Temperature (K)	K_{ads}	$\Delta_{\text{ads}}G^\circ$ (KJ/mol)	$\Delta_{\text{ads}}H^\circ$ (KJ/mol)	$\Delta_{\text{ads}}S^\circ$ (KJ/mol)
P1	308	$3,34.10^4$	-36,98	-10,44	38.89
	318	$6,58.10^4$	-39,98		
	328	$5,92.10^4$	-40,94		
	338	$3,19.10^4$	-40,45		
P2	308	$1,19.10^4$	-40,24	-11,1	36.73
	318	$7,08.10^4$	-40,17		
	328	$4,63.10^4$	-40,27		
	338	$3,35.10^4$	-40,59		
P3	308	$7,64.10^4$	-40,49	-18,3	34,69
	318	$5,14.10^4$	-40,27		
	328	$3,96.10^4$	-40,63		
	338	$3,32.10^4$	-41,01		

In order to continue our study, the parameter of standard enthalpy and standard entropy of inhibition process was calculated from the integrated version of the vant'Hoff isobar expressed by equation (7) [33] and the thermodynamic equation (8) respectively.

$$\ln K_{\text{ads}} = -\frac{\Delta_{\text{ads}}H^\circ}{RT} + cte \quad (7)$$

$$\Delta_{\text{ads}}G^\circ = \Delta_{\text{ads}}H^\circ - T\Delta_{\text{ads}}S^\circ \quad (8)$$

These parameter calculated from the plotting of K_{ads} versus $10^3/T$ showed in figure 8

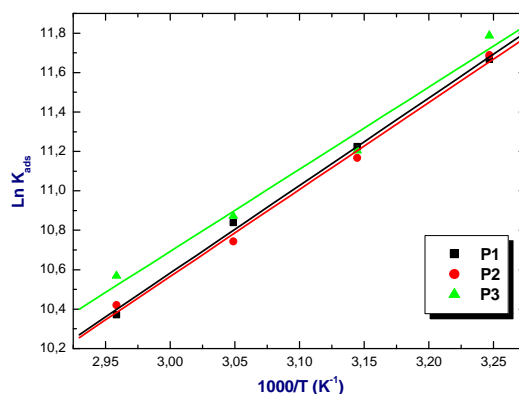


Figure 8. The linear dependence with $\ln K_{\text{ads}}$ versus $1000/T$ for P1, P2 and P3

The negative sign of $\Delta_{\text{ads}}H^\circ$ indicates that the adsorptions of our molecules are an exothermic process. In an exothermic process, physisorption is distinguished from chemisorptions by considering the absolute value of a physisorption process is lower than 40kJ mol^{-1} while the adsorption heat of a chemisorptions process approaches 100kJ mol^{-1} [33]. in our case, the values $\Delta_{\text{ads}}H^\circ$ of our inhibitors are less than 40KJ.mol^{-1} , so we can suggest that P1, P2 and P3 have physisorption process. While the positive values of $\Delta_{\text{ads}}S^\circ$ meaning that our molecules adsorbed onto the mild steel surface with a disordering way.

3.2. Polarization curves

The potentiodynamic polarization curves of C38 steel in HCL 1M in the presence and absence of different concentrations of P1, P2 and P3 are shown in Figure 9. The corresponding electrochemical parameters values of corrosion current densities (I_{corr}), corrosion potential (E_{corr}), cathodic Tafel slope (β_c), anodic Tafel slope (β_a) and inhibition efficiency (EI %) of our molecular are summarized in Table7.

In this case, the inhibition efficiency is defined as following equation:

$$E\% = \frac{I_{corr} - I_{inh}}{I_{corr}} \quad (9)$$

Where I_{corr} and I_{inh} are the corrosion current density values in the absence and presence of inhibitors respectively.

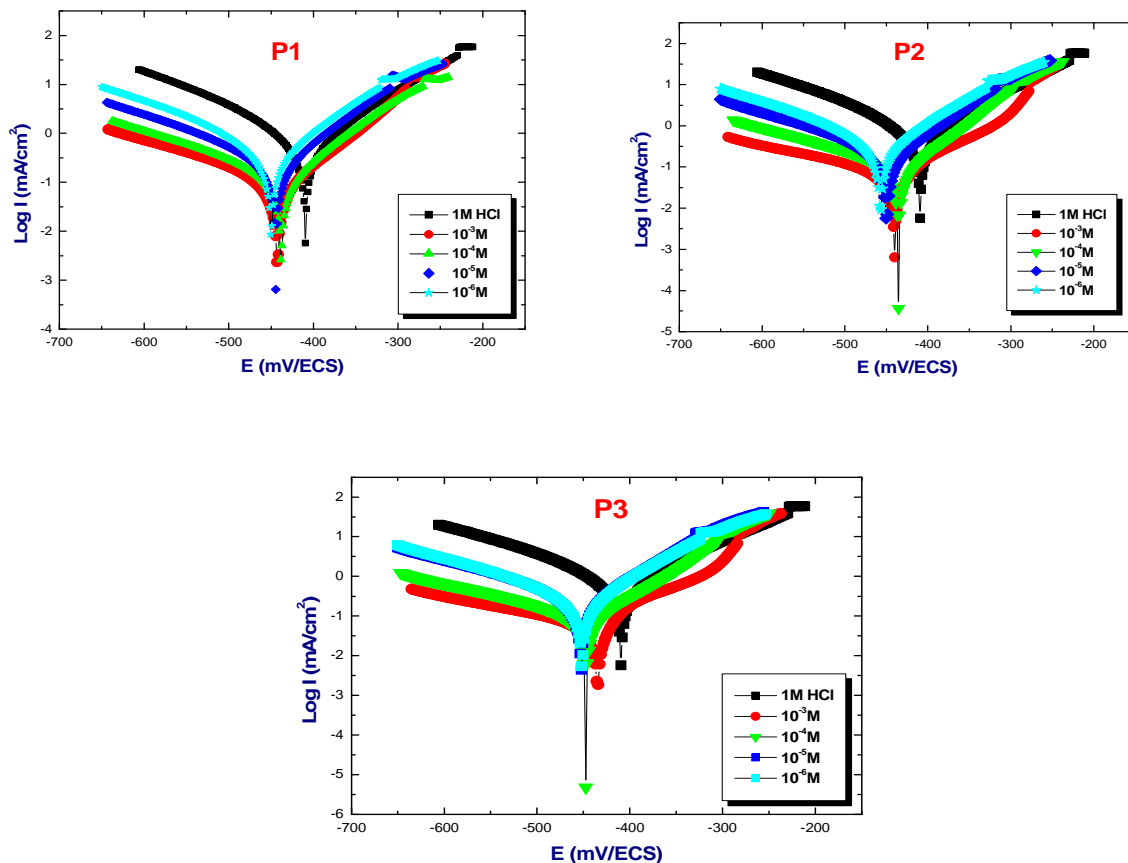


Figure 9: Polarization curves for mild steel in 1 M HCl in the absence and presence of different concentration of P1, P2 and P3

According to Yan et al. [34] an inhibitor can be classified as cathodic or anodic type if the displacement in corrosion potential is more than 85 mV/(SCE), with respect of corrosion potential of the blank. This confirms that our compounds classified as mixed-type inhibitor with predominance cathodic. We also observed that potentials values higher than -350 mV_{ESC}, the compound starts to be desorbed.

Table 7. Potentiodynamic polarization parameters of the stainless steel in HCl solution without and with addition of P1, P2 and P3 at 298K

Inhibitors	Concentration	E (mV/ECS)	I _{corr} (μA.cm ⁻²)	-β _a (mV.dec ⁻¹)	β _c (mV.dec ⁻¹)	E(%)
HCl 1M	--	-406,8	1044,3	117,6	151,5	--
P1	10 ⁻³	439,8	121,9	82,2	203,3	88,32
	10 ⁻⁴	-435,4	153,7	91,6	188,9	85,28
	10 ⁻⁵	-441,9	318,7	95,1	176,3	69,48
	10 ⁻⁶	-447,4	653,1	113,3	176,1	37,46
P2	10 ⁻³	-437,6	71,2	105,2	240,7	93,18
	10 ⁻⁴	-432,9	119,6	75,2	188,6	88,54
	10 ⁻⁵	-447,3	279,5	88,1	171,2	73,23
	10 ⁻⁶	-454,7	536,1	104,8	166	48,66
P3	10 ⁻³	-432	57,1	89,1	227,8	94,53
	10 ⁻⁴	-444,9	105,7	74,1	189,7	89,87
	10 ⁻⁵	-449,9	338,9	86,8	168,5	67,54
	10 ⁻⁶	-448,9	410	90,2	159,4	60,73

The table 7 shows the decrease of the current densities I_{corr} with the increase in P1, P2 and P3 concentration, this decreasing indicates the increased inhibition efficiency of our inhibitor. These results reflect the formation of anodic

protective films containing oxides. We remark also that the efficiency of P3>P2>P1 for the various concentration which can be approved also to the presence of halogenur like Br, Cl, and F in P3 and P2 which favors good adsorption than P1.

3.3. Electrochemical impedance spectroscopy (EIS)

To complete our study, we imply the EIS method. The Figure 10 shows the Nyquist diagrams for synthesized corrosion inhibitor in acid hydrochloric molar at 298K without and with various concentrations of the inhibitors. The high frequency loops are not perfect semicircles which can be attributed to the frequency dispersion as a result of the roughness and inhomogeneous of electrode surface [35]. Moreover, the diameter of the capacitive loop in the presence of inhibitor is bigger than that in the absence of inhibitor (blank solution) and increases with the inhibitor concentration. This indicated that the impedance of inhibited substrate increased with increasing of the corrosion inhibitor concentration. These results show also that the corrosion rate is reduced in the presence of the corrosion inhibitors, at a fixed inhibitor concentration 10^{-3} M, following the order: P3 > P2 >

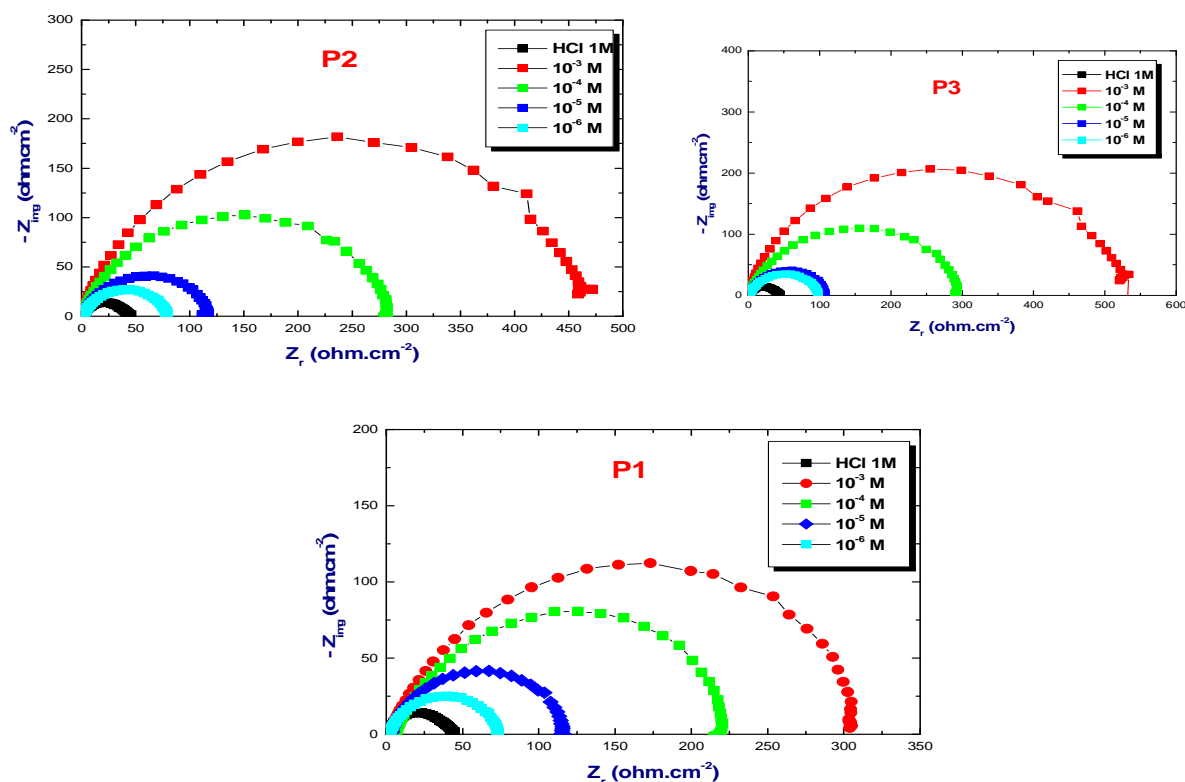


Figure 10. Impedance plot of mild steel obtained in HCl 1M in the absence and presence of various concentrations of inhibitors

The R_{ct} values were used to calculate the inhibition efficiency E% according to the following equation:

$$E\% = \frac{R_{ct} - R_{ct(inh)}}{R_{ct}} * 100 \quad (10)$$

Where R_{ct} and $R_{ct(inh)}$ are respectively the charge transfer resistance in the absence and the presence of inhibitor, respectively. The values of C_{dl} were obtained at f_{max} using equation (11)

$$C_{dl} = \frac{1}{2\pi f_{max} R_{ct}} \quad (11)$$

Table 8. Impedance parameters of mild steel in 1M HCl containing different concentrations of the studied compounds

inhibitors	Concentration (mol.L ⁻¹)	Rt (Ω.cm ²)	Cdl (μF/cm ²)	fmax (Hz)	E (%)
HCl 1M	--	41,04	155	14,15	--
P1	10 ⁻³	320,3	39,74	112,33	87,18
	10 ⁻⁴	229,3	55,51	80,62	82,10
	10 ⁻⁵	117,7	67,57	41,54	65,13
	10 ⁻⁶	72,85	87,38	24,87	43,66
P2	10 ⁻³	469,9	21,4	181,95	91,26
	10 ⁻⁴	287,3	35	102,65	85,71
	10 ⁻⁵	120,5	66,02	41,28	65,94
	10 ⁻⁶	79,21	80,36	26,78	48,18
P3	10 ⁻³	535,8	18,76	206,58	92,34
	10 ⁻⁴	300,8	33,43	109,68	86,35
	10 ⁻⁵	110,7	71,84	41,21	62,92
	10 ⁻⁶	99,4	80,02	34,67	58,71

From the impedance data (table 8) we conclude that the value of R_{tc} increases with increasing of concentration of inhibitors which indicates also an increase in the corrosion efficiency to attain maximum values of 92.34, 91.26 and 87.18% at 10⁻³M for P3, P2 and P1 respectively.

The impedance of Nequist representation was analyzed by fitting the experimental data to a simple equivalent circuit model shows in Figure 11. This circuit as a solution resistance R_s which placed in serie with the double layer capacitance C_{dl} and the charge transfer resistance R_{ct} , which is in parallel.

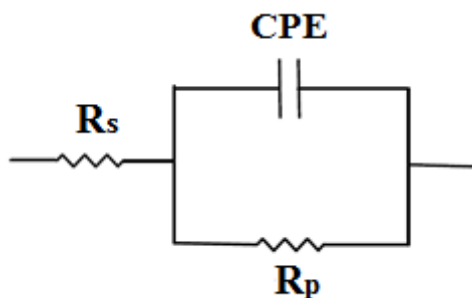


Figure 11. Equivalent electrical circuit model corresponding to the corrosion process on the carbon steel in hydrochloric acid

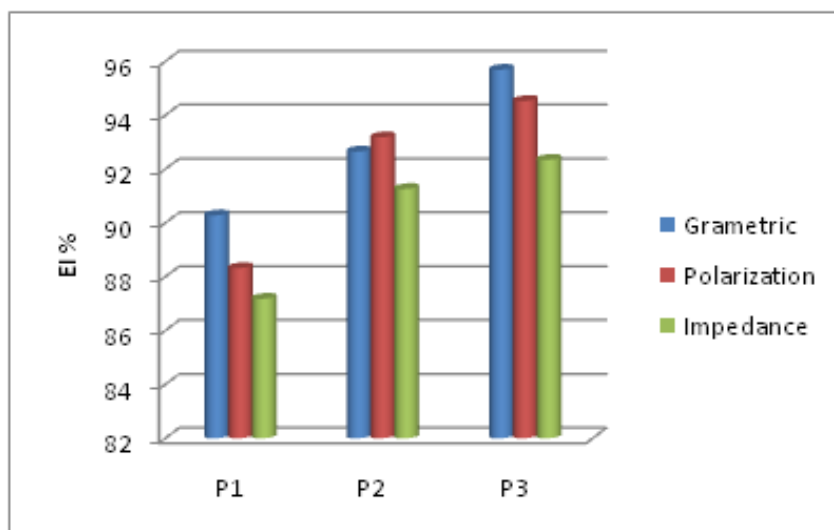


Figure 12. Inhibition efficiency of different inhibitors in HCl 1M

A comparison may be made between inhibition efficiency E (%) values obtained by different methods (weight loss, polarization curves and EIS methods). Figure 12 shows a histogram that compares the E (%) values obtained. One can see that whatever the method used, no significant changes are observed in E (%) values. We can then conclude

that there is a good correlation with the three methods used in this investigation at all tested concentrations and those inhibitors is an efficient corrosion inhibitor.

3.4. Scanning electron microscopic (SEM)

Beside the weight loss measurement and electrochemical test, the surface analysis is too important to show if our inhibitors adsorbed into the specimens surface or not. SEM photographs were obtained after immersion of specimens surface in solution during 6h with and without the optimum concentration of inhibitors (Figure 13-14).

The Figure 13 indicates the finely polished characteristic surface of mild steel although the presence of some scratches due to polishing. (a) and the strongly damaged in the absence of inhibitors due to the direct attack of aggressive acids (b). By comparing the fig 13 to fig 14, it appears that mild steel surface is free from corrosion in HCl solution. This is due to the formation of an adsorbed film of P1, P2 and P3 on the surface. This shows that the inhibitor inhibits corrosion of mild steel in 1 M HCl solution.

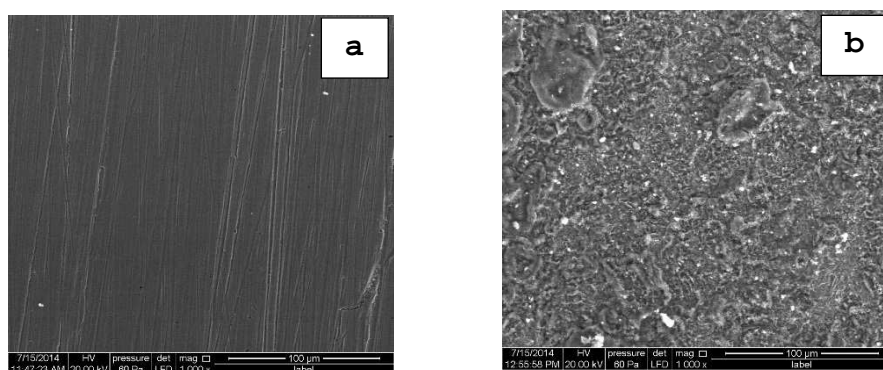


Figure 13. SEM image of mild steel surface (a) before and (b) after 6 hours of immersion in 1M HCl solution in the absence of inhibitors

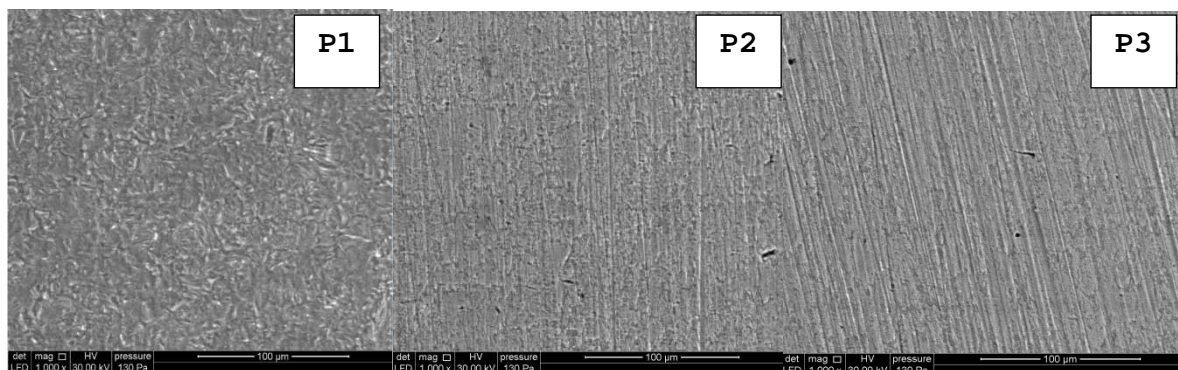


Figure 14. SEM image of mild steel after 6 hours of immersion in 1M HCl solution with 10^{-3} M of inhibitor P1, P2 and P3

CONCLUSION

The following conclusion can be drawn from this study:

- Our molecular are a good inhibitors for steel in HCl 1M especially P3.
- The inhibition efficiency increase with an increase of inhibitive concentration to attains 95% for P3 at 10^{-3} M.
- P1, P2 and P3 act as mixed type with predominance cathodic.
- The three inhibitors adsorbed on the steel surface according to the Langmuir isotherm.
- Gravimetric, Polarization and Impedance methods are in a good agreement for all inhibitors.
- These results confirm that our compounds are both physi and chemisorption mechanism.

REFERENCES

- [1] D. Ben Hmamou, R. Salghi, A. Zarrouk, H. Zarrok, B. Hammouti, S. S. Al-Deyab, A. El Assry, N. Benchat, M. Bouachrine *Int. J. Electrochem. Sci.*, **2013**, 8, 11526 – 11545.
- [2] Y. AitAlbrimi, A. AitAddi, J. Douch, M. Hamdani1, R.M. Souto *Int. J. Electrochem. Sci.*, **2016**, 11, 385 – 397
- [3] S. Shahabi, P. Norouzi, M. Reza Ganjali, *Int. J. Electrochem. Sci.*, **2015**, 10, 2646 – 2662.

- [4] K. Benbouya, B. Zerga, M. Sfaira, M. Taleb, M. EbnTouhami, B. Hammouti, H. Benzeid, E.M. Essassi *Int. J. Electrochem. Sci.*, **2012**, 7, 6313 – 6330.
- [5] W. Niouri, B. Zerga, M. Sfaira, M. Taleb, M. EbnTouhami, B. Hammouti, M. Mcharfi, S.S. Al-Deyab, H. Benzeid, El M. Essassi *Int. J. Electrochem. Sci.*, **2014**, 9, 8283 – 8298.
- [6] M. Belayachi, H. Serrar, H. Zarrok, A. El Assyry, A. Zarrouk, H. Oudda, S. Boukhris, B. Hammouti, Eno E. Ebenso, A. Geunbour. *Int. J. Electrochem. Sci.*, **2015**, 10, 3010 – 3025.
- [7] W. Niouri, B. Zerga, M. Sfaira, M. Taleb, B. Hammouti, M. EbnTouhami, S.S. Al-Deyab, H. Benzeid, El M. Essassi. *Int. J. Electrochem. Sci.*, **2012**, 7, 10190 – 10204.
- [8] D. Ben Hmamou, A. Zarrouk, R. Salghi, H. Zarrok, Eno E. Ebenso, B. Hammouti, M. M. Kabanda, N. Benchat, O. Benali. *Int. J. Electrochem. Sci.*, **2014**, 9, 120 – 138
- [9] N. K. Sebbar, H. Elmsellem, M. Boudalia, S. Iahmidi, A. Belleaouchou, A. Guenbour, E. M. Essassi, H. Steli, A. Aouniti, *J. Mater. Environ. Sci.*, **2015**, 6 (11), 3034-3044.
- [10] M. Messali, A. Bousskri, A. Anejjar, R. Salghi, B. Hammouti. *Int. J. Electrochem. Sci.*, **2015**, 10, 4532 – 4551.
- [11] F. El-Hajjaji, R.A. Belkhemima, B. Zerga, M. Sfaira, M. Taleb, M. EbnTouhami, B. Hammouti, S.S. Al-Deyab and E. Ebenso, *Int. J. Electrochem. Sci.*, **2014**, 9, 4721 – 4731.
- [12] Z. El Adnani, M. Mcharfi, M. Sfaira, M. Benzakour, A.T. Benjelloun, M. EbnTouhami, B. Hammouti, M. Taleb. *Int. J. Electrochem. Sci.*, **2012**, 7, 6738 – 6751.
- [13] Z. El Adnani, A.T. Benjelloun, M. Benzakour, M. Mcharfi, M. Sfaira, T. Saffaj, M. EbnTouhami, B. Hammouti, S.S. Al-Deyab and E.E. Ebenso, *Int. J. Electrochem. Sci.*, **2014**, 9, 4732 – 4746.
- [14] H. Zarrok, A. Zarrouk, R. Salghi, Y. Ramli, B. Hammouti, M. Assouag, E. M. Essassi, H. Oudda and M. Taleb, *J. of Chem. and Pharmaceutical Research*, **2012**, 4(12), 5048-5055
- [15] K. Tebbji, B. Hammouti, H. Oudda, A. Ramdani, M. Benkadour, *applied surface sc*, **2005**, 252, 1378-1385
- [16] A. Elaatioui, Y. Rokni, K. Mohammed, A. Asehraou, T. Chelfi, R. Saddik, A. Oussaid, Jose M. Villalgordo, S. Abouricha, B. El Mahi, A. Oussaid, A. Zarrouk, N. Benchat. *J. Mater. Environ. Sci.*, **2015**, 6 (8), 2083-2088
- [17] M.A. Quraishi and D. Jamal, *Corrosion*, **2000**, 56, 156.
- [18] M. Benabdellah, A. Yahyi, A. Dafali, A. Aouniti, B. Hammouti and A. Ettouhami, *Arab. J. Chem*, **2011**, 4, 343.
- [19] M. Abdallah, H.E. Megahed, M. Sobhi, *Monatshefte fur Chem*, **2010**, 141, 1287.
- [20] M. Mousavi, M. Mohammadalizadeh, A. Khosravan, *Corros. Sci.*, **2011**, 53, 3086.
- [21] A. Chetouani, B. Hammouti, K. Medjahed, A. Mansri, *Der Pharma Chemica*, **2011**, 3, 307.
- [22] K. Bouhrira, F. Ouahiba, D. Zerouali, B. Hammouti, M. Zertoubi, N. Benchat, *E-J Chem* **2010**, 7, 35.
- [23] L. Wang, *Corros. Sci.*, **2006**, 48, 608.
- [24] M. Scendo, *Corros. Sci.*, **2008**, 50, 1584.
- [25] I. Langmuir, *J. Am. Chem. Soc.*, **1947**, 39, 1848.
- [26] J. Flis, T. Zakroczymski, *J. Electrochem. Soc.*, **1996**, 143 (8), 2458-2464.
- [27] M.A. Migahed, *Mater. Chem. Phys.*, **2005**, 93, 48.
- [28] T. Szauer, A. Brand, *Electrochim. Acta*, **1981**, 26, 1219.
- [29] B. Zerga, B. Hammouti, M. EbnTouhami, R. Tourir, M. Taleb, M. Sfaira, M. Bennajeh, I. Forssal. *Int. J. Electrochem. Sci.*, **2012**, 7, 471 – 483.
- [30] A. Popova, E. Sokolova, S. Raicheva, M. Christov, *Corros. Sci.*, **2003**, 45, 33.
- [31] O. Riggs, I. R. Hurd, M. Ray, *Corrosion*, **1967**, 23, 252.
- [32] I. ElOuali, B. Hammouti, A. Aouniti, Y. Ramli, M. Azougagh, E.M., Essassi, M. Bouachrine, *J. Mater. Environ. Sci.*, **2010**, 1, 1.
- [33] Y. Filali Baba, H. Elmsellem, Y. Kandri Rodi, H. Steli, C. AD, Y. Ouzidan, F. Ouazzani Chahdi, N. K. Sebbar, E. M. Essassi, B. Hammouti, *Der Pharma Chemica*, **2016**, 8(4), 159-169.
- [34] Y. Yan, W. Li, L. Cai, B. Hou, *Electrochim. Acta*, **2008**, 53, 5953.
- [35] M. Lebrini, M. Lagrenee, H. Vezin, M. Traisnel, F. Bentiss, *Corros. Sci.*, **2007**, 49, 2254.